*Proc. Natl. Acad. Sci. USA*
Vol. 92, pp. 8026–8030, August 1995
Neurobiology

# Rapid acquisition of dendritic spines by visual thalamic neurons after blockade of *N*-methyl-D-aspartate receptors

**(neuronal activity/development/plasticity/lateral geniculate nucleus/ferret)**

MONICA ROCHA* AND MRIGANKA SUR†

Department of Brain and Cognitive Sciences, Massachusetts Institute of Technology, Cambridge, MA 02139

*Communicated by Emilio Bizzi, Massachusetts Institute of Technology, Cambridge, MA, May 10, 1995*

**ABSTRACT** ***N*-Methyl-D-aspartate (NMDA) receptors play an important role in the development of retinal axon arbors in the mammalian lateral geniculate nucleus (LGN). We investigated whether blockade of NMDA receptors *in vivo* or *in vitro* affects the dendritic development of LGN neurons during the period that retinogeniculate axons segregate into on-center and off-center sublaminae. Osmotic minipumps containing either the NMDA receptor antagonist D-2-amino-5-phosphonovaleric acid (D-APV) or saline were implanted in ferret kits at postnatal day 14. After 1 week, LGN neurons were intracellularly injected with Lucifer yellow. Infusion of D-APV *in vivo* led to an increase in the number of branch points and in the density of dendritic spines compared with age-matched normal or saline-treated animals. To examine the time course of spine formation, crystals of 1,1′-dioctadecyl-3,3,3′,3′-tetramethylindocarbocyanine perchlorate were placed in the LGN in brain slices from 14- to 18-day-old ferrets. Labeled LGN cell dendrites were imaged on-line in living slices by confocal microscopy, with slices maintained either in normal perfusion medium or with the addition of D-APV or NMDA to the medium. Addition of D-APV *in vitro* at doses specific for blocking NMDA receptors led to a >6-fold net increase in spine density compared with control or NMDA-treated slices. Spines appeared within a few hours of NMDA receptor blockade, indicating a rapid local response by LGN cells in the absence of NMDA receptor activation. Thus, activity-dependent structural changes in postsynaptic cells act together with changes in presynaptic arbors to shape projection patterns and specific retinogeniculate connections.**

The mammalian lateral geniculate nucleus (LGN) undergoes considerable change in structure and circuitry during development. In cats, retinal ganglion cell axons from the two eyes initially overlap but become restricted prenatally to discrete termination zones within the LGN according to the eye of origin (1, 2). The visual pathway of ferrets is similar to that of cats in both structure and developmental timing. However, because ferrets are born 3 weeks earlier than cats, the segregation of retinal axons into eye-specific laminae occurs postnatally, between birth and the second postnatal week (3). In addition, during the third postnatal week, on- and off-center retinogeniculate axons from each eye segregate further into inner and outer sublaminae, respectively (4, 5).

The rearrangement of terminal arbors that occurs during development of the mammalian visual system is sharpened by neural activity (6). When neural activity is blocked by the application of tetrodotoxin, retinal axons carrying information from the two eyes remain intermixed within the LGN (7, 8). There is increasing evidence that activity through *N*-methyl-D-aspartate (NMDA) receptors, a subtype of glutamate receptors, plays a critical role in the development of afferent projections in the mammalian visual system (9). In the ferret's visual pathway, blockade of NMDA receptors on postsynaptic cells in the LGN during the third postnatal week prevents the segregation of retinal axons into on- and off-center sublaminae (5). NMDA receptor blockade in the superior colliculus of postnatal rats leads to the retention of aberrant branches at nontopographic locations on retinocollicular axons (10).

While the effect of NMDA receptor blockade on the development of presynaptic afferent axons has been well documented, much less is known about whether NMDA receptors regulate changes in the morphology of target cells themselves during development. We have investigated this issue in the ferret LGN by two separate but complementary approaches. We first examined the effect of NMDA receptor blockade on LGN cell dendrites *in vivo* during the third postnatal week, when retinogeniculate axons segregate into on- and off-center sublaminae, and found a major increase in dendritic branching and spines. We then examined how rapidly the addition of dendritic spines could be observed after receptor blockade *in vitro*, in slices from animals in the third postnatal week, and found that LGN neurons started to acquire dendritic spines within hours after NMDA receptor blockade. These results constitute direct evidence of a clear and rapid role for NMDA receptors in shaping the dendritic structure of neurons in the visual pathway.

## MATERIALS AND METHODS

Timed pregnant ferrets were purchased from Marshall Farms (North Rose, NY), and litters were born in our colony. Twenty-five ferret kits ranging from postnatal day 14 (P14) to P21 were used.

***In Vivo* Blockade of NMDA Receptors and Intracellular Labeling of LGN Neurons.** *Implant of osmotic minipumps.* Ferret kits at P14 were anesthetized with ketamine (4 mg/100 g of body weight) supplemented with methoxyflurane (Metofane, 1–2%). Osmotic minipumps (Alzet model 2001; infusion rate, 1 μl/hr; Alza) containing either 0.8 mM D-2-amino-5-phosphonovaleric acid (D-APV; Cambridge Research Biochemicals) in 0.9% NaCl (saline; $n = 3$) or saline alone ($n = 3$) were implanted subcutaneously at the base of the neck, as described (ref. 5; this dose of D-APV is effective in preventing the segregation of retinogeniculate axons in ferrets into on- and off-center sublaminae during the same developmental period). Each minipump was connected via a catheter to a 7-mm-long stainless steel cannula (Plastics One, Roanoke, VA), which was then inserted into the thalamus. During the

The publication costs of this article were defrayed in part by page charge payment. This article must therefore be hereby marked "*advertisement*" in accordance with 18 U.S.C. §1734 solely to indicate this fact.

Abbreviations: aCSF, artificial cerebrospinal fluid; D-APV, D-2-amino-5-phosphonovaleric acid; DiI, 1,1′-dioctadecyl-3,3,3′,3′-tetramethylindocarbocyanine perchlorate; LGN, lateral geniculate nucleus; NMDA, *N*-methyl-D-aspartate; P*n*, postnatal day *n*.

*Present address: Departamento de Neurobiologia, Instituto de Biofisica–CCS-B1.G, Universidade Federal do Rio de Janeiro, Brazil CEP 21941-590.

†To whom reprint requests should be addressed at: Department of Brain and Cognitive Sciences, Massachusetts Institute of Technology, E25-618, Cambridge, MA 02139.

same procedure, rhodamine-labeled latex microspheres (Lumafluor, New York) were injected into the primary visual cortex (two or three injections, 0.2 μl each) to retrogradely label LGN cells. In normal control animals, the tracer was injected into visual cortex at either P7 ($n = 4$) or P14 ($n = 3$) and the animals were examined at P14 or P21, respectively. Without direct knowledge of drug concentration in the LGN, we chose not to use L-APV as a control for D-APV.

*Slice preparation and cell labeling.* Animals were deeply anesthetized with sodium pentobarbital (35 mg/kg) and transcardially perfused with cold oxygenated artificial cerebrospinal fluid (aCSF: 126 mM NaCl/3 mM KCl/1.25 mM $NaH_2PO_4$/10 mM dextrose/20 mM $NaHCO_3$/1.2 mM $MgSO_4$/2.5 mM $CaCl_2$, pH 7.4, when saturated with 95% $O_2$/5% $CO_2$). The brain was quickly removed, and the cortex and hippocampus were dissected away. The brain chunk containing the thalamus was placed in a cutting dish and submerged in cold aCSF, and 300-μm-thick horizontal slices were cut with a Vibratome (Technical Products, St. Louis). Slices were maintained on nylon baskets submerged in continuously oxygenated aCSF at room temperature. The cannula and catheter connected to the osmotic minipump were tested to ensure that they were free-flowing; animals in which these were blocked were not used further. Individual slices of the thalamus containing the LGN were placed in an interface slice chamber mounted on the stage of an Olympus microscope equipped for epifluorescence. Slices were partially submerged under continuously oxygenated aCSF (1 ml/min) and maintained at room temperature for 2–4 hr. Additional oxygenation was provided by a humidified mixture of 95% $O_2$/5% $CO_2$ inside the chamber.

Glass electrodes were made from thin wall capillary tubing (WPI) and then bent to allow vertical penetration (11). The electrode tip was partially filled with a 20% (wt/vol) solution of Lucifer yellow (Sigma) in 0.1 M LiCl, and the electrode was subsequently filled with 0.1 M LiCl. With a ×10 long-working distance objective (Olympus), rhodamine-labeled cells in the A or A1 lamina of the LGN were located under a rhodamine filter. After a cell was impaled, Lucifer yellow was iontophoretically injected with negative rectangular current pulses (2–20 nA, 1–4 Hz) for a variable time (a few seconds to several minutes), depending on the age of the animal and size of the dendritic arbor. Cells were considered completely filled when bright fluorescence was observed at terminal dendrites.

*Tissue processing and morphometric analysis.* After several LGN neurons were labeled, slices were fixed in 4% paraformaldehyde/0.1 M phosphate buffer, pH 7.4, for 24 hr. The slices were then mounted onto gelatinized slides, flattened, and dehydrated (11). After being photographed at several magnifications, LGN cells were drawn by use of a camera lucida attached to a Leitz Diaplan microscope with a ×100 oil-immersion objective. These drawings (at a final magnification of approximately ×1250) were analyzed with a morphometry system (SigmaScan; Jandel, San Rafael, CA). For statistical analyses, the Mann–Whitney $U$ test was applied (StatView 512+; Brain Power, Calabasas, CA).

Cells were included for quantitative analysis when their dendritic arbors were labeled up to their tips and were contained fully within the slice. Dendritic arbor area was measured as the area within the outermost branch tips of dendrites. Dendritic length was the total length of dendrites for a cell. A branch point was defined as any point of bifurcation in the dendritic tree. Spines were defined as fine dendritic appendages shorter than 3 μm (see ref. 12). Spine density (no. per mm) was calculated from the sum of all spines in a cell divided by the total dendritic length.

***In Vitro* Blockade of NMDA Receptors and Imaging of Dendritic Spines.** *Imaging dendrites in slices.* Ferret kits ranging in age from P14 to P18 were deeply anesthetized with sodium pentobarbital (35 mg/kg, i.p.) and perfused intracardially with cold oxygenated aCSF. Horizontal 400-μm-thick thalamic slices were prepared as described above. Crystals of 1,1′-dioctadecyl-3,3,3′,3′-tetramethylindocarbocyanine perchlorate (DiI; Molecular Probes) 100–300 μm in diameter were immediately placed at multiple locations in the LGN. Slices were kept submerged in continuously oxygenated aCSF at room temperature for 2 hr to allow dye uptake by LGN cells. Individual slices were then placed in a slice chamber mounted on the stage of an upright compound fluorescence microscope (Zeiss Axioplan). Slices were partially submerged under continuously oxygenated aCSF and secured to the bottom of the chamber with a nylon net. Labeled cells and processes were imaged by laser confocal microscopy (Bio-Rad MRC-600) with a ×40 water-immersion objective (Zeiss) with a numerical aperture of 0.75. DiI fluorescence was obtained by 514-nm argon ion laser excitation, with standard filters. With a ×9 electronic zoom, one pixel in the resulting image corresponded to 0.046 μm in the object plane, providing a field of view of 23 μm × 35 μm. A total of 160 dendritic segments, generally 20–35 μm in length (mean, 31.9 ± 1.5 μm), were identified and imaged. At least 5 serial optical sections were collected at 0.5-μm depth intervals through each segment. Each image was the average of 15–20 frames, subsequently processed for contrast stretch. In control experiments, the same segments of dendrites were imaged again after an interval of 2–7 hr. Otherwise, after the first set of images, the solution was changed to aCSF containing either D-APV (50–100 μM) or NMDA (10–100 μM), and the dendritic segments were imaged again after 2–7 hr of perfusion. Electrophysiological recordings showed that LGN cells in thalamic slices kept in a similar chamber remained healthy for ≥12 hr (13, 14).

*Data analysis.* All measurements were made with the MRC-600 confocal microscope operating software (COMOS version 6.03). Spines were short dendritic appendages 0.5–3 μm in length. In a histogram of appendage size, they formed a population clearly distinct from dendritic branches (data not shown). Two images of each dendritic segment collected 2–7 hr apart were compared, and the number of spines added or eliminated was counted. The percent of images in which there was a net increase in spines ("spines added"), a net decrease ("spines eliminated"), or no change was calculated (see Table 2). The increase (or decrease) in spine density was calculated from the number of spines added (or eliminated) in each imaged segment and the length of dendrite imaged. The goal was to examine whether treatment with D-APV or NMDA led to an appreciable effect on dendritic spines compared with control slices observed for similar time periods. We thus confined our analysis to measuring the number and density of spines. Statistical comparisons were done with the $\chi^2$ test and the Mann–Whitney $U$ test.

## RESULTS

**Effect of NMDA Receptor Blockade *in Vivo*.** LGN cells in normal ferrets undergo considerable morphological change during the period that retinogeniculate arbors segregate into laminae and sublaminae (12). We labeled LGN cells intracellularly with Lucifer yellow in living slices in order to reveal fine details of their dendritic structure (Fig. 1). From birth until P14, dendritic arbors increased substantially in area, in arbor complexity (assayed by the number of dendritic branch points), and in the number and density of spines and dendritic appendages (ref. 15; data not shown). By P21, LGN cells had acquired many of the characteristics of adult cells, and morphological cell types could be distinguished (Fig. 1 *a* and *b*).

When NMDA receptors on LGN cells were blocked during the third postnatal week by chronic infusion of D-APV, the dendritic morphology of these cells was markedly altered. The treatment had no effect on soma sizes or dendritic arbor areas of LGN cells examined at P21 (Fig. 1 *c* and *d*; Table 1) but caused cells to have significantly more branch points and spines

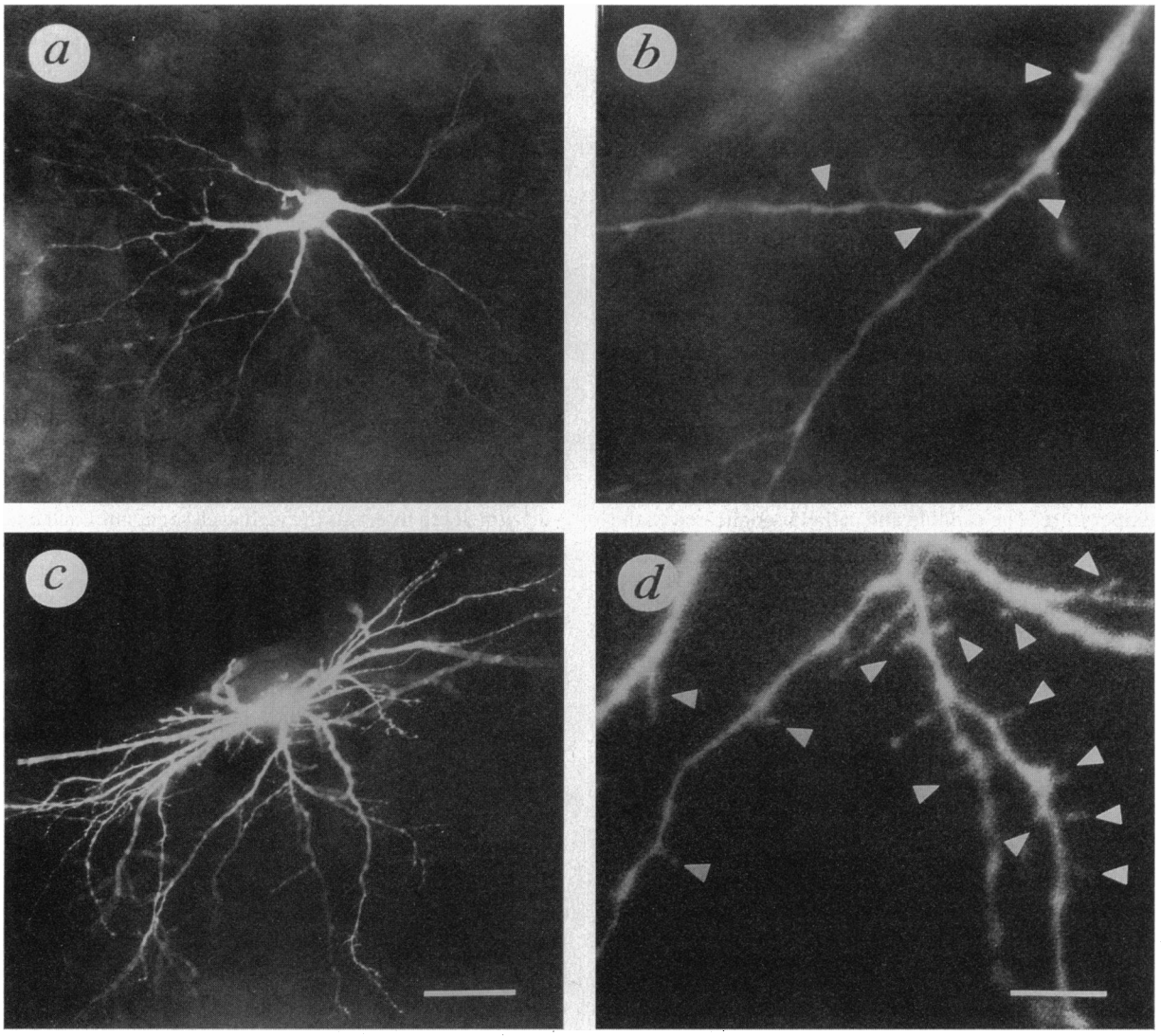


FIG. 1. Photomicrographs of LGN cells filled with Lucifer yellow in P21 ferrets. (*a*) Cell from a normal P21 ferret showing the pattern of branching and density of spines characteristic of type 1 cells at this age. (*b*) Higher magnification of a portion of the dendritic arbor from the same cell. Only a few dendritic spines (arrowheads) can be observed. (*c*) Type 1 cell from a ferret in which D-APV was infused into the thalamus for 1 week from P14 to P21. Blockade of NMDA receptors during the third postnatal week causes LGN cells to have increased branching and markedly increased number of spines. (*d*) Portion of the dendritic arbor from *c* viewed at higher magnification. Dendrites are studded with numerous spines (arrowheads). [Bar in $c = 50$ $\mu$m (applies also to *a*); bar in $d = 10$ $\mu$m (applies also to *b*).]

than cells from normal, untreated animals ($P < 0.001$ for each comparison). Dendritic length and spine density also increased ($P < 0.05$ for each). Similarly, when compared with cells from saline-treated animals, cells from D-APV-treated animals had more dendritic branches and spines ($P < 0.001$ for each), as well as greater spine density ($P < 0.005$) (Table 1). (Cells in saline-treated animals turned out to have fewer spines and lower spine density when compared with cells from normal animals, but were very similar to normal in soma area, dendritic arbor area, dendritic length, and branching. Both groups included the various LGN cell types.) Spines were not distributed evenly over all branches in the dendritic arbor but were concentrated on roughly 60% of branches. When spine density was calculated by considering only branches with spines, the increase in D-APV-treated animals compared with normal animals was even greater (mean of 124.4 ± 14.9 spines per mm in D-APV-treated animals vs. 54.3 ± 6.8 spines per mm in normal animals; $P < 0.001$). These data indicate that a major effect of NMDA receptor blockade during the period of sublamina formation is to increase the number and density of dendritic spines on LGN cells.

**Effect of NMDA Receptor Blockade *in Vitro*.** To determine how rapidly spines formed, we imaged dendrites on-line in living slices *in vitro*, under more controlled conditions of

Table 1. LGN cell morphology in normal, D-APV-treated, and saline-treated ferrets

| Condition | No. of animals | No. of cells | Soma area, $\mu m^2$ | Dendritic arbor area, $\mu m^2 \times 10^{-3}$ | Dendritic length, mm | No. of branch points | No. of spines | Spine density, no./mm |
|---|---|---|---|---|---|---|---|---|
| P14, normal | 4 | 15 | 157.7 ± 13.7 | 27.3 ± 2.8 | 2.3 ± 0.2 | 52.3 ± 4.5 | 109.6 ± 27.1 | 43.1 ± 9.7 |
| P21, normal | 3 | 16 | 171.3 ± 13.4 | 35.0 ± 4.4 | 2.3 ± 0.2 | 44.1 ± 4.2 | 81.6 ± 15.1 | 38.9 ± 6.8 |
| P21, D-APV | 3 | 20 | 167.4 ± 12.4 | 48.1 ± 5.9 | 3.6 ± 0.4 | 79.6 ± 7.7 | 198.4 ± 28.6 | 59.9 ± 6.9 |
| P21, saline | 3 | 7 | 156.9 ± 18.9 | 32.0 ± 12.7 | 2.0 ± 0.5 | 42.7 ± 7.0 | 29.6 ± 9.1 | 19.8 ± 7.6 |

Values are shown as mean ± SE.

observation (Fig. 2 *a* and *b*). Dendrites could be distinguished from axons by their larger-diameter, sometimes tortuous, processes attached to somata and by the presence of spines (Fig. 2). Within a few hours of NMDA receptor blockade, new spines were readily observed (Fig. 2 *c–f*).

Spines were added to or eliminated from dendritic segments imaged in both control and NMDA-treated slices as well as in D-APV-treated slices. We determined the net increase or decrease in spines in individual segments under these different conditions (Table 2). There was a significantly greater proportion of dendritic segments from D-APV-treated slices in which spines were added compared with segments from control or NMDA-treated slices ($P < 0.001$ for each comparison, $\chi^2$ test). In contrast, the proportion of segments showing spine elimination was very similar in D-APV-treated and control or NMDA-treated slices (Table 2). The lack of a significant effect on spine elimination when slices are perfused with NMDA might be due to desensitization of NMDA receptors (16) or possibly to toxic effects that follow continuous application of NMDA (17), though obvious effects were not visible (cell damage could be demonstrated by raising bath temperature or altering ion concentrations in the bath significantly).

Converting the number of spines added or eliminated in each imaged dendritic segment to changes in spine density (Fig. 3), we observed that D-APV perfusion led to a large increase in the density of spines added (37.7 ± 5.2 spines per mm; $n = 70$ segments) when compared with control slices (7.8 ± 2.1 spines per mm; $n = 67$ segments) or NMDA-treated slices (7.3 ± 3.6 spines per mm; $n = 23$ segments; Fig. 3 *Left*). D-APV or NMDA had no effect on spine elimination (Fig. 3 *Center*). Thus, blockade of NMDA receptors led to a >6-fold net increase in spine density compared with control (from 5.7 ± 2.5 to 34.9 ± 5.5 spines per mm; Fig. 3 *Right*; $p < 0.001$ comparing images from D-APV-treated slices and either control or NMDA-treated slices, $P < 0.01$ pooling data from each animal into a single observation). Overall, therefore, about 30 spines per mm were added to LGN cell dendrites within 2–7 hr of NMDA receptor blockade (Fig. 3 *Right*; increase in spine density in D-AVP-treated slices over control slices). For comparison, the overall increase in spine density observed with NMDA receptor blockade *in vivo* was 21–40 spines per mm (Table 1, increase in spine density in P21 D-APV-treated animals over P21 normal or P21 saline-treated animals). Thus, while spine turnover must also occur, most of the increase in spine density under NMDA receptor blockade *in vivo* can be accounted for by spines acquired within a few hours after start of the blockade.

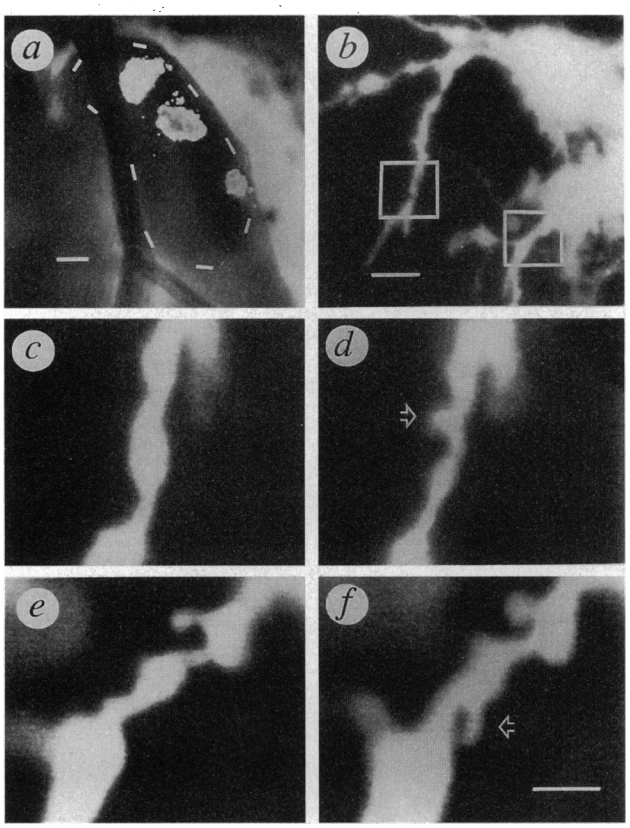


FIG. 2. Laser confocal fluorescence microscopy images of DiI-labeled dendrites of LGN cells in a living thalamic slice from a P16 ferret kit. (*a*) Low-magnification image showing three crystals of DiI placed on the LGN in a 400-μm-thick horizontal thalamic slice. Dashed line indicates the borders of the LGN; dark vertical stripe is a piece of nylon netting used to hold the slice down. (*b*) LGN cells labeled with DiI after 2 hr of incubation. The boxes at left and right show dendritic segments shown at higher power in *c* and *d* and in *e* and *f*, respectively. (*c–f*) Higher magnification of a dendritic segment collected before (*c* and *e*) and 3 hr after (*d* and *f*) the slice was perfused with 100 μM D-APV. Arrows in *d* and *f* point to dendritic spines that appeared after D-APV perfusion. [Bar in *a* = 200 μm; bar in *b* = 10 μm; bar in *f* = 2 μm (applies to *c–f*).]

Table 2. Changes in dendritic spines in control, D-APV-treated, and NMDA-treated slices

| Condition | No. of animals | No. of cells | No. of dendritic segments | % dendritic segments: Spines added | Spines eliminated | No change |
|---|---|---|---|---|---|---|
| Control | 5 | 29 | 67 | 22 | 5 | 73 |
| D-APV | 5 | 25 | 70 | 56 | 3 | 41 |
| NMDA | 2 | 9 | 23 | 17 | 9 | 74 |

## DISCUSSION

Our results indicate that infusion of D-APV into the ferret LGN during the third postnatal week leads to pronounced changes in the dendritic morphology of LGN cells: they have more branches, greater length of dendrites, and an increased density of spines when compared with normal age-matched controls. While we infer that the concentration of D-APV in the LGN following minipump infusion *in vivo* would specifically block NMDA receptors (see ref. 5), it is difficult to rule out nonspecific effects of the drug on other receptor types. At least the increase in spine density occurs rapidly within a few hours of blockade, as observed *in vitro* with concentrations of D-APV known to specifically block NMDA receptor-mediated responses in the ferret LGN (14, 18–20). These data constitute

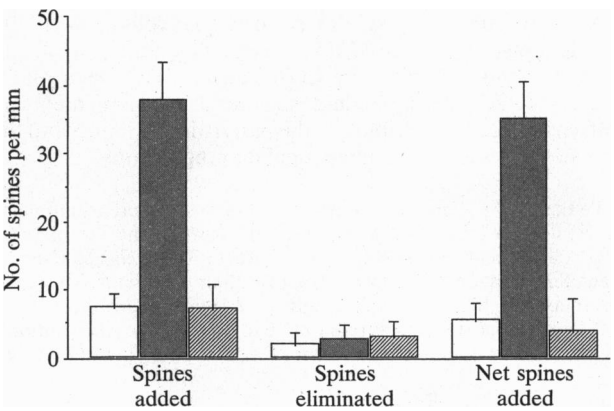


FIG. 3. Changes in spine density (no. of spines per mm) on LGN cells in control slices (open bars) and slices treated with D-APV (50–100 μM) (solid bars) or NMDA (10–100 μM) (hatched bars). Each set of bars shows the increase (spines added), decrease (spines eliminated), and net increase (net spines added) in spine density under each condition.

a clear demonstration of the effect of NMDA receptors on the structure of target neurons in a pathway where these receptors are known to be involved in synaptic transmission and plasticity (14, 18) and in afferent arbor segregation (5).

The activity-dependent regulation of the dendritic structure of LGN cells that we have observed in ferrets occurs before eye-opening and is driven by spontaneous rather than visual activity (21, 22). Blockade of NMDA receptors might specifically disrupt the detection of coincident afferent and target activity in the LGN (9) and, more generally, reduce retinogeniculate transmission and the activity of postsynaptic cells (14, 20). Blockade of NMDA receptors in the ferret LGN during the same developmental period disrupts the segregation of on- and off-center retinogeniculate afferents into sublaminae (5). Individual arbors either remain abnormally large or are of normal size but inappropriately positioned within the LGN. Our finding that LGN cells upregulate their dendritic spines in concert indicates that the development of both pre- and postsynaptic elements of retinogeniculate synapses during this time period depends on neuronal activity mediated by NMDA receptors.

Direct and indirect evidence suggests that afferent activity and synaptic transmission are important for regulating dendritic morphology in the retinogeniculate pathway during development. The density of dendritic spines on LGN cells increases in postnatal ferrets before decreasing to adult levels (12). In the absence of retinal axons (following early eye enucleation), the elimination of transient dendritic spines on LGN cells is delayed (23). Lid suture in postnatal kittens leads to abnormal dendritic structure of LGN cells (24). Intracranial infusion of tetrodotoxin in fetal cats leads to a large increase in the density of LGN cell dendritic spines (25). In the developing retina, blocking the release of glutamate by bipolar cells prevents the normal stratification of retinal ganglion cell dendrites (26), and blockade of NMDA receptors leads to an increase in the number of dendritic spines on these neurons (27).

Dendritic spines represent a major target of excitatory synapses on spiny neurons in the visual pathway, including cells in the LGN (ref. 28; but see ref. 29). The rapid addition of spines on LGN neurons following blockade of NMDA receptors suggests that an active cellular mechanism leading to the formation of dendritic spines is negatively regulated by afferent activity. The intracellular mechanisms that direct this regulation are likely to involve intracellular calcium (30–34), which might subsequently mediate phosphorylation of proteins, regulation of protein synthesis, or local gene expression (35–37). NMDA receptors influence dendritic outgrowth in isolated hippocampal neurons (38, 39) and cause rapid alterations in the actin cytoskeleton of cerebellar cells *in vitro* (40). Our demonstration that NMDA receptors regulate the acquisition of dendritic spines by LGN neurons suggests strongly that rapid, activity-dependent structural rearrangements in postsynaptic cells contribute to the patterning of inputs and the formation of specific retinogeniculate connections.

We thank Ary Ramoa and Jong-on Hahm for their contributions to the *in vivo* blockade experiments, Suzanne Kuffler and David Smith for excellent technical assistance, and Rafael Linden, Karina Cramer, Diana Smetters, and Francisco Clasca for their comments. This study was supported by a National Institutes of Health grant (EY07023). M.R. was supported by a research fellowship from the National Council for Development of Science, Brazil.

1. Hickey, T. L. & Guillery, R. W. (1974) *J. Comp. Neurol.* **156,** 239–254.
2. Shatz, C. J. (1983) *J. Neurosci.* **3,** 482–499.
3. Linden, D. C., Guillery, R. W. & Cucchiaro, J. (1981) *J. Comp. Neurol.* **203,** 189–211.
4. Stryker, M. P. & Zahs, K. R. (1983) *J. Neurosci.* **3,** 1943–1951.
5. Hahm, J., Langdon, R. B. & Sur, M. (1991) *Nature (London)* **351,** 568–570.
6. Shatz, C. J. (1990) *Neuron* **5,** 745–756.
7. Shatz, C. J. & Stryker, M. P. (1988) *Science* **242,** 87–89.
8. Sretavan, D. W., Shatz, C. J. & Stryker, M. P. (1988) *Nature (London)* **336,** 468–471.
9. Constantine-Paton, M., Cline, H. T. & Debski, E. (1990) *Annu. Rev. Neurosci.* **13,** 129–154.
10. Simon, D. K., Prusky, G. T., O'Leary, D. D. M. & Constantine-Paton, M. (1992) *Proc. Natl. Acad. Sci. USA* **89,** 10593–10597.
11. Ramoa, A. S., Campbell, G. & Shatz, C. J. (1988) *J. Neurosci.* **8,** 4239–4261.
12. Sutton, J. K. & Brunso-Bechtold, J. K. (1991) *J. Comp. Neurol.* **309,** 71–85.
13. White, C. A. & Sur, M. (1992) *Proc. Natl. Acad. Sci. USA* **89,** 9850–9854.
14. Esguerra, M., Kwon, Y. H. & Sur, M. (1992) *Visual Neurosci.* **8,** 545–555.
15. Rocha, M. & Sur, M. (1992) *Soc. Neurosci. Abstr.* **18,** 1310.
16. Chizhmakov, I. V., Kistin, N. I. & Krishtal, J. (1992) *J. Physiol. (London)* **448,** 453–472.
17. Choi, D. W. (1991) in *Glutamate: Cell Death and Memory*, eds. Ascher, P., Choi, D. W. & Christen, Y. (Springer, Berlin), pp. 125–136.
18. Mooney, R., Madison, D. V. & Shatz, C. J. (1993) *Neuron* **10,** 815–825.
19. Ramoa, A. S. & McCormick, D. A. (1994) *J. Neurosci.* **14,** 2089–2097.
20. Ramoa, A. S. & McCormick, D. A. (1994) *J. Neurosci.* **14,** 2098–2105.
21. Galli, L. & Maffei, L. (1988) *Science* **242,** 90–91.
22. Meister, M., Wong, R. O. L., Baylor, D. A. & Shatz, C. J. (1991) *Science* **252,** 939–943.
23. Sutton, J. K. & Brunso-Bechtold, J. K. (1993) *J. Neurobiol.* **24,** 317–334.
24. Friedlander, M. J., Stanford, L. R. & Sherman, S. M. (1982) *J. Neurosci.* **2,** 321–330.
25. Dalva, M. B., Ghosh, A. & Shatz, C. J. (1994) *J. Neurosci.* **14,** 3588–3602.
26. Bodnarenko, S. R. & Chalupa, L. M. (1993) *Nature (London)* **364,** 144–146.
27. Lau, K. C., So, K. & Tay, D. (1992) *Brain Res.* **595,** 171–174.
28. Wilson, J. R., Friedlander, M. J. & Sherman, S. M. (1984) *Proc. R. Soc. London B* **221,** 411–436.
29. Wong, R. O. L., Yamawaki, R. M. & Shatz, C. J. (1992) *Eur. J. Neurosci.* **4,** 1387–1397.
30. Muller, W. & Connor, J. A. (1991) *Nature (London)* **354,** 73–76.
31. Guthrie, P. B., Segal, M. & Kater, S. B. (1991) *Nature (London)* **354,** 76–79.
32. Koch, C. & Zador, A. (1993) *J. Neurosci.* **13,** 413–422.
33. Desmond, N. L. & Levy, W. B. (1986) *J. Comp. Neurol.* **253,** 466–475.
34. Harris, K. & Stevens, J. K. (1989) *J. Neurosci.* **9,** 2982–2997.
35. Brostom, C. O. & Brostom, M. A. (1990) *Annu. Rev. Physiol.* **52,** 577–590.
36. Torre, E. R. & Steward, O. (1992) *J. Neurosci.* **12,** 762–772.
37. Chicurel, M. E., Terrian, D. M. & Potter, H. (1993) *J. Neurosci.* **13,** 4054–4063.
38. Brewer, G. J. & Cotman, C. W. (1989) *Neurosci. Lett.* **99,** 268–273.
39. Mattson, M. P. (1988) *Brain Res. Rev.* **13,** 179–212.
40. Rashid, N. A. & Cambray-Deakin, M. A. (1992) *Dev. Brain Res.* **67,** 301–308.